Improved singum model based on finite deformation of crystals with the thermodynamic equation of state

Huiming Yin[1]

[1]Associate Professor, Dept. of Civil Engineering and Engineering Mechanics, Site Director of Center for Energy Harvesting Materials and System, Columbia University, 610 Seeley W. Mudd 500 West 120th Street, New York, 10027. Email: yin@civil.columbia.edu

ABSTRACT

The recently published simplified singum model has been improved by using the thermodynamics-based equation of state (EOS) of solids to derive a new interatomic potential based on the elastic constants. The finite deformation formulation under hydrostatic load has been used to evaluate the pressure-volume (p-v) relationship for the EOS of a solid. Using the bulk modulus and its derivatives at the free-stress state, one can construct the EOS, from which a new form of interatomic potential is derived for the singum, which exhibits much higher accuracy than the previous one obtained from the Fermi energy and provides a general approach to construct the interatomic potential. The long-range atomic interactions are approximated to be proportional to the pressure. This improved singum model is demonstrated for the face-centered cubic (FCC) lattice of single crystalline aluminum. The elastic properties at different pressures are subsequently predicted through the bond length change and compared with the available experimental data. The model can be straightforwardly extended to higher order terms of EOS with better accuracy and other types of lattices.

INTRODUCTION

In the recent paper (Yin 2022b), a continuum particle model, namely the singum model, was presented to simulate an atomic lattice with singular interatomic forces by a continuum particle system with stresses through particle's interfaces. The Wigner-Seitz (WS) cell (Wigner and Seitz 1933) is used to construct the singum particles through the Voronoi decomposition of a crystal lattice (Voronoi 1908). Although a point force in a continuum solid is a strong singularity that exhibits an infinite displacement or stress in continuum mechanics, an isotropic stress-strain relationship can be established with the aid of the Fermi energy for bulk modulus (Shukla 1981) by the homogenization of stress over the singum's volume and orientation. Therefore, the two independent isotropic elastic constants can directly map to the two constants in the interatomic potential given the crystal lattice characteristics (Yin 2022b). However, the simple form of the Fermi energy cannot capture the general pressure-volume relation over finite deformation and was proposed to be replaced by a polynomial form (Johnson 1972; Shukla 1981).

The equation of state (EOS) of solids describes the volume or density change of solids under an increasing hydrostatic pressure over a large range (Vinet et al. 1989; Cohen et al. 2000). Birch (Birch 1952) classified the EOS in four groups: 1) quantum mechanics uses the atomic constants to predict the elastic constants at at (absolute) zero temperature; 2)the Fermi energy approximates a solid as an electron gas, subject to the Fermi-Dirac statistics, and predicts the p-v relationship; 3) the semi-empirical laws of cohesion with the temperature-dependent energy predict the relationship among temperature, pressure and density of solids, and; 4) thermodynamics provides a general framework to predict the elasticity with the parameters to be calibrated by other means.

Although the Fermi energy could provide reasonable prediction of elasticity through the calibration with the elastic constants (Yin 2022b), the accuracy was not high for general solids. The EOS based on the thermodynamic equation is typically provided in form of the Helmholtz free energy, which correlates the state variables, such as pressure, volume, temperature, or internal energy (Fürth 1944; Birch 1952). It provides more flexibility to calibrate the parameters for high accuracy and has been well accepted in the research community (Birch 1952).

Although elastic solids are often assumed with the linearity of the stiffness by the Hooke's law, the experimental data under large pressure (Guinan and Steinberg 1974; Holzapfel et al. 2001; Occelli et al. 2003) showed the significant change of compressibility with pressure. Birch (Birch 1947) used Murnaghan's finite deformation theory (Murnaghan 1937) to consider the effect of pressure upon the second-order elastic constants and obtained excellent comparisons with the experiments for compressibility of solids, which is coined as the Murnaghan-Birch's (MB) EOS. Although many forms of EOS have been proposed and used for specific solids (Cohen et al. 2000; Occelli et al. 2003; Swift et al. 2022), the MB EOS is still widely used for its robustness and simplicity. Under the general loading condition, the thermodynamics-based framework can provide a practical approach to predicting the nonlinear elastic behavior of atomic lattices (Wei et al. 2009; Tadmor and Miller 2011).

The singum model provides a clear approach to correlate the interatomic potential with the elasticity at the undeformed state and the EOS of the solids (Yin 2022b). It was generalized to lattice metamaterials and composites for prediction of the effective elasticity based on the stiffness of the lattice components and the structure of the lattice using a harmonic potential (Yin 2022a). This is the third paper in this series to extend the formulation to finite deformation under hydrostatic loading and thus correlate the nonlinear elastic behavior of crystals with the interatomic potential in a rigorous way. Particularly, because the interatomic potential function plays a significant role on the chemistry and physics of materials (Jarvis et al. 1996; Ruiz et al. 2015; Zuo et al. 2020; Mishin 2021), it is critical to find an accurate interatomic potential.

Based on the two previous papers, a crystal lattice is simplified into continuously packed singum particles with short-range particle interaction forces equal to the interatomic forces. Along the surface, the atoms form a surface layer and interact with the inner singums. The atomic interactions in the surface layer are different from those between the singums and produce a prestress to the lattice, so that the undeformed state of the crystals exhibit a bond length different from the equilibrium bond length. By applying a displacement variation, from the variations of the stress and strain, one can derive the stiffness explicitly, and therefore establish the relationship

between the stiffness of the crystal and the potential between atoms. When the solid is under a high pressure, the lattice exhibits a hydrostatic deformation while keeping the same lattice structure, but the stiffness of the lattice changes with the bond length. The formulation (Yin 2022b) developed with infinitesimal strain is not sufficient to catch the nonlinear material behavior under finite deformation of hydrostatic loading. This paper improves the singum model with a new form of the interatomic potential and addresses some confusing issues in the first paper (Yin 2022b), which will be clarified subsequently.

In the remainder of this paper, we firstly revisit the assumptions of the singum model (Yin 2022b) and use the finite deformation to formulate the pressure-volume (p-v) relationship and constitutive law, and then derive a new singum potential function based on the MB EOS of solids with other elastic constants at the undeformed state. The modeling method can also be extended to other forms of EOS obtained from either experiments or theories. Given a singum potential and the crystal lattice characteristics, the tangential elastic constants can be calculated at a given material state. The model is demonstrated for face-centered cubic (FCC) lattices of single crystalline aluminum. The comparison with the experimental results shows the capability and accuracy of the model.

FORMULATION

This section we use a face-centered cubic (FCC) lattice as an example to formulate the problem, which can be generalized to other lattices. We will first derive the MB EOS based on the singum configuration, then set up the constitutive equation in terms of the interatomic potential, and finally derive the EOS based singum potential. Based on the previous work (Yin 2022b; Yin 2022a), a freestanding lattice may exhibit a prestress due to the surface energy of the atom interaction on the boundary, so that the bond length $2l_p^u$ in the undeformed state can be different from the equilibrium bond length $2l_p^0$ of two freestanding atoms. Here the bond length $2l_p^0$ refers to the minimal potential energy, which is used as the reference coordinate $\mathbf{X}$, and other states can be represented by $\mathbf{x}$ with a deformed bond length $2l_p$. The freestanding lattice is represented by $\mathbf{x}^u$ with the bond length $2l_p^u$.

The equation of state of the singum

Consider an FCC crystal lattice in Fig. 1(a). In the reference configuration, the unit cell of an FCC lattice exhibits the cubic edge length a^0, so that the bond length $2l_p^0 = \frac{a^0}{\sqrt{2}}$, where the interatomic force of the bonds is zero and kinetic energy of atoms is not considered. We set up the coordinate with the origin at the 0^{th} atom, and 12 closest neighbor atoms are located at $(\pm\frac{a^0}{2}, \pm\frac{a^0}{2}, 0)$, $(\pm\frac{a^0}{2}, 0, \pm\frac{a^0}{2})$, $(0, \pm\frac{a^0}{2}, \pm\frac{a^0}{2})$, which are corresponding to the directional vectors $\mathbf{n}^I$ $(I = 1, 2, ..., 12) = (\pm\frac{1}{\sqrt{2}}, \pm\frac{1}{\sqrt{2}}, 0)$, $(\pm\frac{1}{\sqrt{2}}, 0, \pm\frac{1}{\sqrt{2}})$, or $(0, \pm\frac{1}{\sqrt{2}}, \pm\frac{1}{\sqrt{2}})$.

Following the previous paper (Yin 2022b), we can construct the singum particle by cutting the 12 bonds with the vertical midplanes forming a rhombic dodecahedron in Fig. 1(b), in which F^7 shows the bond force between the 0^{th} and 7^{th} atoms as an example of the 12 bonds to be cut at the midpoint by a perpendicular plane. Both Figs. 1(a) and (b) shows the bond force of atom 0-7 acting at the cutting point. Notice that two unit cells are needed to construct the singum illustrated in Fig. 1(b) with four atoms on the interfac and four in each unit cell. A Cartesian coordinate $\mathbf{X}$ is setup at the zero-force bond length, i.e. the Lagrangian coordinates. After a homogeneous deformation of the lattice, the material points in $\mathbf{X}$ are referred to $\mathbf{x}$ at the deformed state, or the Eulerian coordinates, in which the lattice still keeps periodic, so that the whole space can still be filled with the deformed singums. Here because the singum is defined by the bonds, each surface will still keep plane. The central symmetry of the lattice can be observed, so that the atoms keep in equilibrium under the deformation. Without any loss of generality, the origins of $\mathbf{x}$ and $\mathbf{X}$ are both selected at the center of Atom 0.

The displacement field is written as $\mathbf{u} = \mathbf{x} - \mathbf{X}$. The deformation gradient tensor is defined as $F_{ik} = \frac{\partial x_i}{\partial X_k}$. The finite strain can be defined either in the Lagrangian coordinates as $E_{ij} = \frac{1}{2}(F_{ki}F_{kj} - \delta_{ij})$ or in the Eulerian coordinates as $\varepsilon_{ij} = \frac{1}{2}(\delta_{ij} - F_{ki}^{-1}F_{kj}^{-1})$ (Hutter and Jöhnk 2013; Bazant and Cedolin 2010). Because the stress or pressure is typically measured at the Eulerian coordinates, the latter is used for consistence:

$$\varepsilon_{ij} = \frac{1}{2}[\delta_{ij} - (\delta_{ki} - u_{k,i})(\delta_{kj} - u_{k,j})] = \frac{1}{2}(u_{i,j} + u_{j,i} - u_{k,i}u_{k,j}) \tag{1}$$

Applying a hydrostatic load p, we can test the equation of state from the p-v curve (Birch 1947). Due to the central symmetry, the bond length $2l_p$ of all bonds will uniformly change, namely the deformed length $r = 2l_p\lambda$, where λ is the stretch ratio of the bond. An isotropic strain is obtained from Eq. (1) in corresponding to a hydrostatic load as:

$$\varepsilon_{ij} = \epsilon\delta_{ij} \tag{2}$$

where $\epsilon = \frac{1}{2}\left[2\frac{\lambda-1}{\lambda} - \frac{(\lambda-1)^2}{\lambda^2}\right] = \frac{1}{2}(1-\lambda^{-2})$ by using $u_{i,j} = \frac{\lambda-1}{\lambda}$. The volume ratio of the singum is written as

$$\frac{v_0}{v} = \lambda^{-3} = (1-2\epsilon)^{3/2} \tag{3}$$

where v and v_0 represent the deformed volume and initial volume, respectively.

Following Birch's assumption (Birch 1947; Birch 1952), the Helmohotz free energy of the singum under a hydrostatic load alone can be written in terms of the finite strain as

$$\Psi = a\epsilon^2 + b\epsilon^3 + c\epsilon^4 + \cdots \tag{4}$$

where a, b, c are the second, third, fourth-order elastic constants depending on temperature only. It can be extended to higher order terms, but typically when up to third order terms are used, the EOS produces fairly accurate results for general solids. Specifically, a is related to the bulk modulus, b and c are related to the pressure derivative of the bulk modulus, which will be discussed subsequently. Then the pressure can be written as

$$p = -\frac{d\Psi}{d\epsilon}\frac{d\epsilon}{dv} = -\frac{1}{3v_0}(1-2\epsilon)^{5/2}(2a\epsilon + 3b\epsilon^2 + 4c\epsilon^3 + \cdots) \tag{5}$$

Using Eq. (3), the above equation can be further simplified into

$$p = \frac{a}{3v_0}(\lambda^{-7} - \lambda^{-5})\left[1 - \frac{3b}{4a}(\lambda^{-2}-1) + \frac{c}{2a}(\lambda^{-2}-1)^2\right] \tag{6}$$

where the higher order terms are disregarded. Given the atomic weight M_a, we can calculate the density, namely ρ_0, of the solid as

$$\rho_0 = \frac{M_a}{v_s^0} = \frac{M_a}{4\sqrt{2}l_p^3} \tag{7}$$

where $v_s^0 = 4\sqrt{2}l_p^3$ is the singum's initial volume for FCC lattices in Fig. 1(a). The conservation of the mass also implies

$$\rho/\rho_0 = v_s^0/v_s = \lambda^{-3} \tag{8}$$

Therefore, the MB EOS of Eq. (6) can be equivalently written in terms of density ratio as well (Birch 1952).

From the above relationship, the bulk modulus changing with λ can be derived as

$$\begin{aligned} k(\lambda) =& -\frac{dp}{dv/v} = -v\frac{dp}{d\lambda}\frac{d\lambda}{dv} \\ =& \frac{a}{9v_0}\Big\{(7\lambda^{-7} - 5\lambda^{-5})\left[1 - 0.75b/a(\lambda^{-2}-1) + 0.5c/a(\lambda^{-2}-1)^2\right] \\ &+ (\lambda^{-9} - \lambda^{-7})\left[-1.5b/a + 2c/a(\lambda^{-2}-1)\right]\Big\} \end{aligned} \tag{9}$$

When $\lambda = 1$, the following relations are obtained by Eqs. (6) and (9) as:

$$k_0 = \frac{2a}{9v_0}; \quad k_0' = \frac{dk}{dp}|_{\lambda=1} = 4 - \frac{b}{a}; \quad k_0'' = \frac{d^2k}{dp^2}|_{\lambda=1} = \frac{\frac{12c}{a} - 9k_0'^2 + 63k_0' - 143}{9k_0} \tag{10}$$

Therefore, the parameters of a, b, c in Eqs. (6) and (9) can be written in terms of the bulk modulus and its pressure derivatives of k_0, k_0', k_0'' with more clear physical meanings as follows

$$a = \frac{9v_0k_0}{2}; \quad \frac{b}{a} = 4 - k_0'; \quad \frac{c}{a} = \frac{3}{4}\left(k_0k_0'' + k_0'^2 - 7k_0' + \frac{143}{9}\right) \tag{11}$$

so that Eqs. (6) and (9) can be rewritten as

$$p = \frac{3k_0}{2}(\lambda^{-7} - \lambda^{-5})\left[1 + \frac{3}{4}(k_0' - 4)(\lambda^{-2}-1) + \frac{3}{8}\left(k_0k_0'' + k_0'^2 - 7k_0' + \frac{143}{9}\right)(\lambda^{-2}-1)^2\right] \tag{12}$$

and

$$k(\lambda) = \frac{k_0}{2}\left\{(7\lambda^{-7} - 5\lambda^{-5})\left[1 + \frac{3}{4}(k_0' - 4)(\lambda^{-2} - 1) + \frac{3}{8}\left(k_0 k_0'' + k_0'^2 - 7k_0' + 143/9\right)(\lambda^{-2} - 1)^2\right]\right.$$
$$\left. + \frac{3}{2}(\lambda^{-9} - \lambda^{-7})\left[(k_0' - 4) + \left(k_0 k_0'' + k_0'^2 - 7k_0' + 143/9\right)(\lambda^{-2} - 1)\right]\right\} \tag{13}$$

The above $p - v$ relation is the well-known Murnaghan-Birch (MB) EOS (Birch 1947; Birch 1952). Although the above equations can be extended to the terms higher than 4th order of $c\epsilon^4$ (Wei et al. 2009) in the similar fashion of the above procedure, as most crystals crack or the lattice is distorted when λ changes too far from 1, the higher order terms play less important role, and the improvement of the higher-order EOS was not significant. If only the second order term of $a\epsilon^2$ is considered, we can obtain $k_0' = 4, k_0'' = -\frac{35}{9k_0}$ by using $b = c = 0$. Then only one constant of k_0 is taken into account and the EOS becomes

$$p^a(\lambda) = \frac{3k_0}{2}(\lambda^{-7} - \lambda^{-5}) \tag{14}$$

and

$$k^a(\lambda) = \frac{k_0}{2}\left[\frac{7}{\lambda^7} - \frac{5}{\lambda^5}\right] \tag{15}$$

Very often people used up to the third order terms with $a\epsilon^2 + b\epsilon^3$ or k_0, k_0' to fit the experimental curves (Hama and Suito 1996; Cohen et al. 2000) and the corresponding EOS can be written as

$$p^b(\lambda) = \frac{3k_0}{2}(\lambda^{-7} - \lambda^{-5})\left[1 + \frac{3}{4}(k_0' - 4)(\lambda^{-2} - 1)\right] \tag{16}$$

and

$$\begin{aligned} k^b(\lambda) =& \frac{k_0}{2}\left\{(7\lambda^{-7} - 5\lambda^{-5})\left[1 + \frac{3}{4}(k_0' - 4)(\lambda^{-2} - 1)\right] + \frac{3}{2}(\lambda^{-9} - \lambda^{-7})(k_0' - 4)\right\} \\ =& \frac{k_0}{2}\left[\left(\frac{k_0'}{4} - 1\right)\frac{27}{\lambda^9} - \left(\frac{3k_0'}{2} - 7\right)\frac{7}{\lambda^7} + \left(\frac{3k_0'}{4} - 4\right)\frac{5}{\lambda^5}\right] \end{aligned} \tag{17}$$

For reference, the Fermi energy provides $k(\lambda) = \frac{k_0}{\lambda^2}$ instead (Yin 2022b), which is fairly different

from the above MB-EOS. Note that the thermodynamic EOS refers to the zero-stress configuration that the short-range interatomic potential reaches the minimal with a bond length $2l_p^0$ and the bond force is zero. However, in the actual crystal, the surface energy may produce prestress in the atomic lattice, such as surface tension, so that the bond length $2l_p^u$ of the crystal at the undeformed state can be different from $2l_p^0$.

To make the formulation thermodynamically consistent, we use the zero-stress state as the reference coordinate $\mathbf{X}$, instead of the undeformed state of the crystal, namely $\mathbf{x}^u$, for the following finite deformation formulation, which clarifies some confusing issues in the previous paper (Yin 2022b).

The constitutive relation with the incremental displacement

Because the resultant interatomic force on Atom 0 is zero due to the equilibrium, no body force exists on the singum. Therefore, the Cauchy stress on the singum at the Eulerian coordinates (Fig. 1b) satisfies the equilibrium equation in absence of the body force or inertia force as:

$$\sigma_{ij,i} = 0 \tag{18}$$

Due to the cutoff of 12 bonds, the boundary condition is written as

$$\sigma_{ij} n_i = \Sigma_{I=1}^{12} F_j^I \delta(\mathbf{x}\text{-}\mathbf{x}^I) \quad \text{for } \mathbf{x} \in \partial V_S \tag{19}$$

where $\delta(\mathbf{x})$ is a Dirac Delta function. Following the similar procedure (Yin 2022b), the stress integral of the singum can be written as (Mura 1987)

$$S_{ij} = \int_{v_s} \sigma_{ij}(\mathbf{x}) d\mathbf{x} = \int_{\partial v_s} x_i \sigma_{kj} n_k d\mathbf{x} = \Sigma_{I=1}^{12} x_i^I F_j^I \tag{20}$$

where the interatomic force can be written in terms of the derivative of the potential as

$$F_i^I = \frac{\partial V^I}{\partial x_i} = V_{,r}^I n_i \tag{21}$$

The stress integral in Eq. (20) shares the similar form of the internal virial stress (Zhou 2003; Chen and Fish 2006; Jiménez Segura et al. 2022), which has been used to represent the stress integral in a representative volume element (RVE) with many atoms for a convergent estimate. This equation provides an exact form for short-range atomic interactions on periodically distributed atoms.

Although the stress cannot be well-defined on atoms, it can be measured on the singum through the average of the above stress integral as

$$\sigma_{ij} = \frac{S_{ij}}{v_s} \tag{22}$$

where $v_s = \lambda^3 v_s^0$ is the current volume of the singum. Given the stretch ratio of the bond length, $\lambda = l_p/l_p^0$, the average stress of the singum can be calculated from the above equation.

To test the stiffness of the singum at the current configuration given λ in the Eulerian coordinate $\mathbf{x}$, following the Cauchy-Born rule(Ming et al. 2007; Ericksen 2008; Tadmor and Miller 2011), we apply an incremental displacement variation at every field point x

$$\delta u_i(\mathbf{x}) = \delta d_{ki} x_k \tag{23}$$

where $d_{ki} = u_{i,k}$ represents the displacement gradient tensor because the displacement gradient variation $\delta u_{i,j}(\mathbf{x})$ is so small that the higher-term is negligible. The current coordinate at the I^{th} cutoff point x_i^I is written as

$$x_i^I = \lambda l_p n_i^I + \delta u_i^I \tag{24}$$

where the variation of x_i^I due to the displacement variation is written as

$$\delta x_i^I = \delta u_i^I = \delta d_{ki} x_k^I \tag{25}$$

The deformation gradient tensor at x_i^I is given as

$$F_{ij} = \lambda \delta_{ij} + \delta d_{ki} F_{kj} \quad \text{or} \quad F_{ji} = \lambda \left(\delta_{ij} - \delta d_{ij}\right)^{-1} \tag{26}$$

Therefore, one can obtain

$$F_{ji}^{-1} = \lambda^{-1}(\delta_{ij} - \delta d_{ij}) \tag{27}$$

and

$$\varepsilon_{ij} = \frac{1}{2}\left(\delta_{ij} - F_{ki}^{-1}F_{kj}^{-1}\right) = \frac{1}{2}\left(1 - \lambda^{-2}\right)\delta_{ij} + \delta\varepsilon_{ij} \tag{28}$$

where

$$\delta\varepsilon_{ij} = \frac{1}{2\lambda^2}\left(\delta d_{ij} + \delta d_{ji} - \delta d_{ik}\delta d_{jk}\right) \tag{29}$$

in which the higher order term of $\delta d_{ik}\delta d_{jk}$ can be disregarded when δd_{ij} is small. Therefore, the variation of the Eulerian strain is obtained:

$$\delta\varepsilon_{ij} = \frac{\delta d_{ij} + \delta d_{ji}}{2\lambda^2} \tag{30}$$

The incremental stress-strain relation can define the tangential elastic moduli of the solids, which can be derived from the relationship between the variations of the Cauchy stress and Eulerian strain at the current configuration. The volume change caused by δu_i can be written as

$$\delta v_s = \left[(1+\delta d_{11})(1+\delta d_{22})(1+\delta d_{33}) - 1\right] v_s \approx \delta d_{ii} v_s \tag{31}$$

where the higher order terms are ignored because the displacement variations are small. The variation of average stress can be obtained by taking variation of Eq. (22) with the aid of Eqs. (25) and (31)as

$$\begin{aligned}
\delta\sigma_{ij} &= \frac{1}{v_s}\Sigma_{I=1}^{12}\left(x_i^I F_{j,l}^I \delta x_l + \delta x_i^I F_j^I - x_i^I F_j^I \frac{\delta v_s}{v_s}\right) \\
&= \frac{1}{v_s}\Sigma_{I=1}^{12}\left(x_i^I F_{j,l}^I \delta d_{kl} x_k^I + \delta d_{ki} x_k^I F_j^I - x_i^I F_j^I \delta d_{kk}\right) \\
&= \frac{1}{v_s}\Sigma_{I=1}^{12}\left[(\lambda^2 V_{,\lambda\lambda}^{I0} - \lambda V_{,\lambda}^{I0}) n_i^I n_j^I n_k^I n_l^I + \lambda V_{,\lambda}^{I0}(\delta_{il} n_j^I n_k^I + \delta_{jl} n_i^I n_k^I - \delta_{kl} n_i^I n_j^I)\right]\delta d_{kl}
\end{aligned} \tag{32}$$

where $n_i^I = \frac{x_i^I}{|\mathbf{x}^I|}$, $r = 2l_p^0\lambda$ so that $V(r)$ can be re-defined in terms of $V(\lambda)$, and $2l_p^0 V_{,r} = V_{,\lambda}$ and

$(2l_p^0)^2 V_{,rr} = V_{,\lambda\lambda}$. Both forms of $V_{,r}$ and $V_{,\lambda}$ are used in the literature, but the present formulation is much simpler and more elegant with the dimensionless variable λ. The summation in Eq. (32) is reduced to the summation of $n_i^I n_j^I$ and $n_i^I n_j^I n_k^I n_l^I$, which can be written in the following identities for the FCC in Fig. 1,

$$\begin{aligned} \Sigma_{I=1}^{12} n_i^I n_j^I &= 4\delta_{ij} \\ \Sigma_{I=1}^{12} n_i^I n_j^I n_k^I n_l^I &= (1-\delta_{IK})\delta_{ij}\delta_{kl} + (\delta_{ik}\delta_{jl} + \delta_{jk}\delta_{il}) \end{aligned} \tag{33}$$

where the terms with subscript indices including both uppercase and lowercase letters, Mura's extended index notation is used as follows (Mura 1987; Yin and Zhao 2016):

1. Repeated lower case indices are summed up as usual index notation;
2. Uppercase indices take on the same numbers as the corresponding lower case ones, but are not summed.

Therefore, with the aid of Eq. (30), Eq. (32) can be rewritten as:

$$\begin{aligned} \delta\sigma_{ij} &= \frac{1}{v_s}\left[(\lambda^2 V_{,\lambda\lambda} - \lambda V_{,\lambda})[(1-\delta_{IK})\delta_{ij}\delta_{kl} + (\delta_{ik}\delta_{jl} + \delta_{jk}\delta_{il})] + 4\lambda V_{,\lambda}(\delta_{ik}\delta_{jl} + \delta_{jk}\delta_{il} - \delta_{ij}\delta_{kl})\right]\delta d_{kl} \\ &= \frac{\lambda^2}{v_s}\left[(\lambda^2 V_{,\lambda\lambda} - 5\lambda V_{,\lambda})\delta_{ij}\delta_{kl} - (\lambda^2 V_{,\lambda\lambda} - \lambda V_{,\lambda})\delta_{IK}\delta_{ij}\delta_{kl} + (\lambda^2 V_{,\lambda\lambda} + 3\lambda V_{,\lambda})(\delta_{ik}\delta_{jl} + \delta_{jk}\delta_{il})\right]\delta\varepsilon_{kl} \end{aligned} \tag{34}$$

where the superscript $I0$ is ignored as it is the same of $V_{,\lambda\lambda}^{I0}$ and $V_{,\lambda}^{I0}$ for all the bonds ($I = 1, 2, \cdots, 12$) because they exhibit the same length in the FCC lattice. Since δd_{kl} and δd_{lk} produce the same stress states, δd_{kl} can be replaced by $\lambda^2\delta\varepsilon_{kl}$ with the aid of Eq. (30).

Considering the relationship between the variations of average stress and average strain in Eqs. (34), we can obtain the stiffness tensor of the singum as

$$C_{ijkl} = \frac{\lambda^2}{4\sqrt{2}(\lambda l_p^0)^3}\left[(\lambda^2 V_{,\lambda\lambda} - 5\lambda V_{,\lambda})\delta_{ij}\delta_{kl} - (\lambda^2 V_{,\lambda\lambda} - \lambda V_{,\lambda})\delta_{IK}\delta_{ij}\delta_{kl} + (\lambda^2 V_{,\lambda\lambda} + 3\lambda V_{,\lambda})(\delta_{ik}\delta_{jl} + \delta_{jk}\delta_{il})\right] \tag{35}$$

which exhibits a cubic symmetry depending on the interatomic potential function and the geometry

of the lattice or singum. Note that this paper addresses two confusing issues in the first paper (Yin 2022b): 1) the third term in Eq. (32) was dropped off due to the assumption that the virtual displacement does not change the volume; 2) the effect of strech ratio λ to the Eulerian strain and volumetric strain was not considered under the infinitesimal strain assumption. Therefore, Eq. [19] in the reference (Yin 2022b) is different from the above equation. The present equation removes the assumptions and should be used instead. The three independent elastic constants for the cubic symmetric lattice can be written as:

$$c_{11} = \frac{\lambda V_{,\lambda\lambda} + V_{,\lambda}}{2\sqrt{2} l_p^{0\,3}}, \quad c_{12} = \frac{\lambda V_{,\lambda\lambda} - 5V_{,\lambda}}{4\sqrt{2} l_p^{0\,3}}, \quad c_{44} = \frac{\lambda V_{,\lambda\lambda} + 3V_{,\lambda}}{4\sqrt{2} l_p^{0\,3}} \tag{36}$$

where the Voigt notation is used as $c_{11} = C_{1111}, c_{12} = C_{1122}$, and $c_{44} = C_{1212}$.

In comparison with the recent paper (Yin 2022b), because the volume change of the singum is considered for the average stress in Eq. (20) with the finite deformation, the elastic constants c_{11} and c_{12} exhibit different forms. The Cauchy discrepancy exists as $c_{12} - c_{44} \neq 0$, so that it indeed exhibits a cubic symmetry. Note that the stiffness is calculated with the short-range interatomic potential by the cutoff of the bond length, which includes the twelve member atoms only. In this way, the singular force is homogenized into the integral of stress on the singum and the stiffness is clearly defined. When more interatomic forces are considered, such as the atom from outer layers of atoms and the interaction forces among other pairs of atoms, the average virtual stress will be different, and the relation between the elasticity $\mathbf{C}$ and derivatives of V in Eq. (36) will be more complex as more atoms with different interatomic spacing and orientation need to be considered. This issue will be revisited with the long-range atom interactions in the future.

A new singum potential based on the equation of state

Given an interatomic potential, we can predict the elasticity by the above singum model straightforwardly. Actually, the relationship between the elastic constants and the potential also provides feasibility to develop an interatomic potential to directly match them. Note that the three constants in Eq. (36) can be directly measured in experiments. Given the testing configuration with an initial

bond length $2l_p$, referred to the zero stress configuration with the bond length $2l_p^0$, one can obtain $\lambda_0 = l_p/l_p^0$. Particularly, the shear strain in the lattice can distort the relative position of atoms, which may lead to the lattice transformation and singum annihilation when the closest neighboring atoms change. Therefore, we cannot directly use Eq. (36) to inversely derive V.

However, a hydrostatic load causes the uniform change of the lattice structure and the singum remains stable. Therefore, we can use the bulk modulus to construct the new interatomic potential. Given a hydrostatic stress $\sigma^m\delta_{ij}$, from the volumetric strain, we can calculate the bulk modulus as

$$k(\lambda) = \frac{c_{11}+2c_{12}}{3} = \frac{\lambda V_{,\lambda\lambda} - 2V_{,\lambda}}{3\sqrt{2}l_p^{0\,3}} \tag{37}$$

Inversely, $V(\lambda)$ can be written in terms of $k(\lambda)$ by solving the above ordinary differential equation (ODE) as:

$$V(\lambda) = 3\sqrt{2}l_p^{0\,3}\int_1^\lambda \lambda^2\left[\int_1^\lambda \lambda^{-3}k(\lambda)d\lambda + C\right]d\lambda + V(1) \tag{38}$$

where $V(1)$ is the interatomic potential at $\lambda = 1$, which can be disregarded for elastic modeling because it has no effects; C is an integral constant to be determined subsequently, which is zero shown in Eq. (40); $k(\lambda)$ can be given by the EOS of the crystal. In the recent paper (Yin 2022b), we used the assumption of the volume-dependent interatomic energy with the Fermi energy (Shukla 1981; Johnson 1972), i.e. $E_v = P(\overline{V}/\overline{V}_0)^{-2/3}$, to derive the singum potential. There are many analytic and semi-empirical forms of EOS in the literature (Cohen et al. 2000; Vinet et al. 1986; Chen and Chen 1991; Occelli et al. 2003). The MB EOS has been widely used for the simplicity and accuracy. Eqs. (9), (15), or (17) can be used in Eq. (38) to derive the interatomic potential at the desirable accuracy.

For the convenience of derivation, we can write the derivatives of $V(r)$ as

$$\begin{aligned}
\frac{V_{,\lambda}}{3\sqrt{2}l_p^{0\,3}} &= \lambda^2\left[\int_1^\lambda \lambda^{-3}k(\lambda)d\lambda + C\right] \\
\frac{V_{,\lambda\lambda}}{3\sqrt{2}l_p^{0\,3}} &= 2\lambda\left[\int_1^\lambda \lambda^{-3}k(\lambda)d\lambda + C\right] + \lambda^{-1}k(\lambda) \\
\frac{V_{,\lambda\lambda\lambda}}{3\sqrt{2}l_p^{0\,3}} &= 2\left[\int_1^\lambda \lambda^{-3}k(\lambda)d\lambda + C\right] + \lambda^{-2}k(\lambda) + \lambda^{-1}k_{,\lambda}(\lambda)
\end{aligned} \tag{39}$$

where Eq. (37) can be confirmed by substituting the first two equations into it.

Note that $V_{,\lambda}$ shows the force between two atoms. The physical meaning of C can be described by the interatomic force at the zero-stress state from the first equation in Eq. (39) as:

$$C = \frac{V_{,\lambda}|_{\lambda=1}}{3\sqrt{2}l_p^{0\,3}} = 0 \tag{40}$$

where V reaches the minimum at $\lambda = 1$. Then substituting Eq. (39) into Eq. (36) yields

$$\begin{aligned}
c_{11}(\lambda) &= \frac{3}{2}\left[k(\lambda) + 3\lambda^2\int_1^\lambda \lambda^{-3}k(\lambda)d\lambda\right] \\
c_{12}(\lambda) &= \frac{3}{4}\left[k(\lambda) - 3\lambda^2\int_1^\lambda \lambda^{-3}k(\lambda)d\lambda\right] \\
c_{44}(\lambda) &= \frac{3}{4}\left[k(\lambda) + 5\lambda^2\int_1^\lambda \lambda^{-3}k(\lambda)d\lambda\right]
\end{aligned} \tag{41}$$

Therefore, given the bond length $2l_p^0$ at the zero stress state or the reference coordinate $\mathbf{X}$ and the EOS or $k(\lambda)$, one can obtain the elastic constants changing with the bond length λ or pressure.

Inversely, if three elastic constants c_{11}^u, c_{12}^u and c_{44}^u are measured at λ^u or bond length at $2l_p^u$, the formulation may provide an approach to back calculate the bond length ratio $\lambda^u = l_p^u/l_p^0$ and the EOS $V(\lambda)$ if the form is predefined. However, because only the short range atomic interactions are considered for the atoms with the shortest bond length, the above calculation may not be possible. For example, Eq. (36) implies $2c_{11} = c_{12} + 3c_{44}$, which is against the physics that the cubic symmetry exhibits three independent elastic constants.

Overall, it is not accurate to use the simplified singum model with short-range atomic interactions only to back calculate the EOS of crystals, which exhibits long-range atomic interactions. However, for metamaterials, one can fabricate the lattice with only physical bond connections for neighboring nodes only (Yin 2022a), so that the short-range interactions exactly describe the mechanics. The above formulation can predict the nonlinear elastic behavior of the metamaterial lattice, which is more consistent than the formulation in the second paper (Yin 2022a), which calculate the tangential stiffness based on the infinitesimal strain but allows finite deformation of the bond length. When the long-range atomic interaction is considered, higher accuracy is anticipated and the constraint between the cubic elastic constants can be released.

Approximation of the long-range atomic interactions

To consider the effect of the long-range atomic interaction of crystals, an ergodic process of all interaction forces, which rapidly decay with the atom-atom distance, may provide the accurate numerical results. However, it will not be a closed form solution as Eq. (35). Inspired by the embedded atom method (EAM) (Daw and Baskes 1984; Tadmor and Miller 2011), which considered the interactions of long-range atoms by the embedding energy as a function of density of the host (Daw and Baskes 1984), this paper introduces a hydrostatic stress σ^p_{ij} on the singum surface to simulate the effect of all other atoms beyond the singum members as a correction to the whole stress in Eq. (22) as follows:

$$\sigma^p_{ij} = sp(v_s)\delta_{ij} \tag{42}$$

where s is a constant depending on the material to be determined by the elastic constants later, so that the change of σ^p_{ij} is determined by $p(v_s)$ only. Obviously, when $s = 0$, it recovers the short-range model. Note that because the mass of the singum is constant, v_s is related to density by Eq. (8), it can be written as a function of density as well in parallel to EAM.

Given a displacement variation δu as Eq. (25), one can write

$$\delta\sigma^p_{ij} = s\frac{dp}{dv_s}\delta v_s\delta_{ij} = s\frac{dp}{dv_s}v_s\delta d_{kk}\delta_{ij} = -sk(\lambda)\lambda^2\delta\varepsilon_{kk}\delta_{ij} \tag{43}$$

where Eqs. (30) and (31) are used. Therefore, the modified stiffness can be written in parallel to Eqs. (35) and (36) as

$$\overline{C}_{ijkl} = C_{ijkl} - sk(\lambda)\lambda^2\delta_{ij}\delta_{kl} \tag{44}$$

and

$$\overline{c}_{11} = \frac{\lambda\overline{V}_{,\lambda\lambda} + \overline{V}_{,\lambda}}{2\sqrt{2}l_p^{0\,3}} - sk(\lambda)\lambda^2, \quad \overline{c}_{12} = \frac{\lambda\overline{V}_{,\lambda\lambda} - 5\overline{V}_{,\lambda}}{4\sqrt{2}l_p^{0\,3}} - sk(\lambda)\lambda^2, \quad \overline{c}_{44} = \frac{\lambda\overline{V}_{,\lambda\lambda} + 3\overline{V}_{,\lambda}}{4\sqrt{2}l_p^{0\,3}} \tag{45}$$

where the overbar of $(\bar{\cdot})$ shows the relevant quantity considering the long-range atomic interaction.

Using the similar procedure in the last subsection, one can derive the interatomic potential as follows:

$$k(\lambda) = \frac{\lambda\overline{V}_{,\lambda\lambda} - 2\overline{V}_{,\lambda}}{3\sqrt{2}l_p^{0\,3}} - sk(\lambda)\lambda^2 \tag{46}$$

Inversely, $\overline{V}(\lambda)$ can be written in terms of $k(\lambda)$ by solving the above ordinary differential equation (ODE) as:

$$\overline{V}(\lambda) = 3\sqrt{2}l_p^{0\,3}\int_1^\lambda {}^2\left[\int_1^\lambda \lambda^{-3}g(\lambda)d\lambda + C\right]d\lambda \tag{47}$$

where $g(\lambda) = k(\lambda)(1 + s\lambda^2)$. Compared with Eq. (38), the above equation uses $g(\lambda)$ to replace $k(\lambda)$, so that Eq. (39) can be updated in the same fashion. Therefore, Eq. (41) can be rewritten as

$$\begin{aligned}
\overline{c}_{11}(\lambda) &= \frac{3}{2}\left[k(\lambda)(1+s\lambda^2) + 3\lambda^2\int_1^\lambda \lambda^{-3}k(\lambda)(1+s\lambda^2)d\lambda\right] - sk(\lambda)\lambda^2 \\
\overline{c}_{12}(\lambda) &= \frac{3}{4}\left[k(\lambda)(1+s\lambda^2) - 3\lambda^2\int_1^\lambda \lambda^{-3}k(\lambda)(1+s\lambda^2)d\lambda\right] - sk(\lambda)\lambda^2 \\
\overline{c}_{44}(\lambda) &= \frac{3}{4}\left[k(\lambda)(1+s\lambda^2) + 5\lambda^2\int_1^\lambda \lambda^{-3}k(\lambda)(1+s\lambda^2)d\lambda\right]
\end{aligned} \tag{48}$$

If three elastic constants $\overline{c}^u_{11}$, $\overline{c}^u_{12}$ and $\overline{c}^u_{44}$ are measured at λ^u or bond length at $2l^u_p$, the formulation may provide an approach to back calculate the bond length ratio $\lambda^u = l^u_p/l^0_p$, s, and the EOS $V(\lambda)$ as follows:

$$k(\lambda^u) = \frac{\overline{c}^u_{11} + 2\overline{c}^u_{12}}{3}, \quad s = \frac{3}{\lambda^{u2}}\frac{\overline{c}^u_{12} - 2\overline{c}^u_{11} + 3\overline{c}^u_{44}}{\overline{c}^u_{11} + 2\overline{c}^u_{12}} \tag{49}$$

where λ^u must satisfy

$$\lambda^2 \int_1^{\lambda} \lambda^{-3} k(\lambda)(1 + s\lambda^2) d\lambda = \frac{\overline{c}^u_{11} - \overline{c}^u_{21} - \overline{c}^u_{44}}{3} \tag{50}$$

When the form of the EOS $k(\lambda)$ is given, one can use the above equation to solve for λ^u. For example, if Eq. (15) is used, it can be rewritten as

$$k(\lambda) = k(\lambda^u) \frac{7\lambda^{-7} - 5\lambda^{-5}}{7\lambda^{u-7} - 5\lambda^{u-5}} \tag{51}$$

Substituting Eqs. (51) and (49) into Eq. (50) leads to the numerical solution of λ_u. Therefore, the EOS $k(\lambda)$ and the interatomic potential $\overline{V}(\lambda)$ of the crystal can be determined by the elastic constants.

Ideally, given the cubic symmetric elastic constants of an FCC lattice at the undeform state, one can determine the equilibrium bond length l_p^0 by λ^u and the interatomic potential $V(\lambda)$. Note that if higher order EOS is used, such as Eq. (9) or (17) with the pressure derivatives of the bulk modulus, the derivative of the elastic moduli or the elastic moduli at another value of λ shall be used to determine k_0', k_0'', etc.. The similar procedure can be followed to determine the interactomic potential. Assuming $k_0' = 4, k_0'' = -\frac{35}{9k_0}$, Eq. (15) provides the same prediction as Eq. (9) or (17).

RESULTS AND DISCUSSION

Although this simplified singum model only considers the short range interatomic forces with the interactions of other atoms evaluated in an approximate fashion, because the short range interaction indeed dominates in solids, the model can capture the physics and mechanics of solids with good fidelity. Particularly, because the singum interatomic potential is derived and calibrated by the elastic behavior, the accuracy of the model may reach the engineering standard. Obviously, the volume-surface ratio of a continuum particle will play a role on its effective elasticity due to the boundary effect when it is small. However, the lattice structure and effective elasticity of crystals are fairly stable with size reduction to the nanoscale (Juvé et al. 2010). It indicates that the long-range atom interactions play much less important role on the solid states than in the liquid or

gas states. As the interatomic force is applied to any pair of atoms through the pairwise potential, which reduces to zero rapidly with the center-center distance is much higher than the regular bond length, an ergodic process to consider each pair of atoms should be conducted to yield the effective elasticity. However, it is computationally expensive but cannot provide a close-form expression. Therefore, this paper simplifies it with short-range atomic interaction only for the explicit form of equations of the elasticity. It will be extended to the general case with many particles in future work. Instead, the simplified singum model improved by approximation of the long-range atomic interaction provides a practical way to derive both EOS and interatomic potential from the elastic constants. In the following, we use single crystalline aluminum to demonstrate the application and then discuss the mechanics and physics of crystals predicted by the improved singum model and its connections with the previous two papers and existing models.

Demonstration of the singum potential with the aluminum atomic lattice

Aluminum is a common structural material in civil engineering. Here we use the single crystalline aluminum FCC lattice to demonstrate the use of the improved singum model. The cubic symmetric elastic constants at room temperature have been measured as (Vallin et al. 1964):

$$c^u_{11} = 107.3\text{GPa}, \quad c^u_{12} = 60.08\text{GPa}, \quad c^u_{44} = 28.30\text{GPa} \tag{52}$$

In addition, other parameters can be obtained as follows: Density $\rho = 2.710 \times 10^3 \text{Kg/m}^3$; and atom weight $M_a = 4.482 \times 10^{-26}\text{Kg}$. Using the density and atom weight, we can calculate: the bond length $2l^u_p = 0.286\text{nm}$, and the singum volume $v^u_s = 16.54\text{A}^3$.

Using the three elastic constants in Eqs. (48), we obtain:

$$k(\lambda^u) = 75.82, \quad s = -\frac{0.9182}{\lambda^{u2}} \tag{53}$$

For demonstration, the simplest form of EOS (15) is used as

$$k(\lambda) = 75.82 \frac{7\lambda^{-7} - 5\lambda^{-5}}{7(\lambda^u)^{-7} - 5(\lambda^u)^{-5}} \tag{54}$$

Therefore, λ^u can be determined by Eq. (50) approximately at 1.1199. Using $\lambda^u = 1.1199$ in Eq. (54), and then Eq. (47), one can obtain the EOS and the singum potential as follows:

$$\begin{aligned} k(\lambda) &= 229.89(7\lambda^{-7} - 5\lambda^{-5}) \\ \overline{V}(\lambda) &= 8.8307 \times 10^{-30}(29.801\lambda^{-6} - 83.042\lambda^{-4} + 83.979\lambda^{-2} - 35.604 + 4.8654\lambda^3) \end{aligned} \tag{55}$$

where $\overline{V}(1)$ is disregarded as it has no effect on elasticity prediction. The above formulation can reproduce the measured elastic constants by Eq. (48).

Note that λ refers to the free-force bond length $l_p^0 = 0.1277$nm, which represents the singum volume $v_s^0 = 11.77\text{A}^3$. Therefore, $\lambda = (v/11.77)^{1/3}$, the EOS can be rewritten in terms of volume as well:

$$\begin{aligned} k(v) &= 229.89[7(v/11.77)^{-7/3} - 5(v/11.77)^{-5/3}] \\ \overline{p}(v) &= p_0 - \int_{11.77}^{v} k(v)/v dv = p_0 + 689.67[(v/11.77)^{-7/3} - (v/11.77)^{-5/3}] \end{aligned} \tag{56}$$

where $\overline{p}(v)$ denotes the pressure measurement on the surface of the lattice for comparison with the experiments, and due to the surface energy it is different from Eq. (6) with the internal stress only; $p_0 = p(11.77)$ is caused by the surface energy at the zero-force bond length, which can be calibrated as $p_0 = 79.575$GPa by the measurement $\overline{p}(v_s^u) = \overline{p}(16.54) = 0$. Without the surface energy and long-range atomic interactions, the singum should rest at $v_0 = 11.77\text{A}^3$ but the surface tension of p_0 makes the bond stabilized at $v_s^u = 16.54\text{A}^3$ at the undeformed state instead.

Fig. 2 shows the EOS of aluminum predicted with the three elastic constants with the second order EOS Eq. (15); whereas Fig. 3 illustrates the interatomic potential changing with λ with $V(1)$ disregarded. Both figures can predict the undeformed state at 16.54A^3 or $l_p^u = 0.143$nm because the parameters were fitted by the measurements. However, because Eq. (15) assumed $k' = 4, k_0'' = -\frac{35}{9k_0}$ at $v = v_s^0$ to simplify the mathematical form, it may not catch the real physics of the crystal lattice. For EOS, the experimental results (Dewaele et al. 2004) with a pressure up to 144.3GPa are also provided. Obviously, the dash line of Eq. (56) overly estimate the pressure

in comparison with the experiments of aluminum. Although Eq. (15) exhibits the simplicity and convenience for modeling, the predictions shown in dash lines in both figures may only be usable in the neighborhood of the undeformed state for infinitesimal deformation, and the accuracy will decrease for large deformation.

Eq. (17) has often been used and widely accepted in the literature (Birch 1947; Dewaele et al. 2004). Following the same procedure, once a pressure derivative of k' is given, we can determine λ^u, k_0 and the interatomic potential $V(r)$ as well. Therefore, $k' = 2, 3$ are also shown in Fig. 2, which are corresponding to $\lambda^u = 1.1444, 1.1334$, respectively. Apparently, the case of $k' = 2$ as the solid line exhibits the best fitting to the experimental results of the $p - v$ curve and can be used for further analysis of elasticity changing with pressure, such as pressure derivatives of the elastic constants at different pressures. The EOS and the corresponding potential function are written as:

$$p(\lambda) = \frac{1770.9}{\lambda^7} - \frac{1106.8}{\lambda^5} - \frac{664.10}{\lambda^9} + 72.256$$
$$\overline{V}(\lambda) = 8.2755 \times 10^{-30}(-22.640\lambda^{-8} + 102.39\lambda^{-6} - 169.35\lambda^{-4} + 129.33\lambda^{-2} - 44.558 + 4.8270\lambda^3) \tag{57}$$

Note that the case of $k' = 2$ does not ideally catch the experiments yet at the high pressures in Fig. 2. If Eq.(9) is used with k'' variable to fit the curve, higher accuracy is expected. Compared the above equation with Eq. (56) and (55), the prestress p_0 becomes smaller with one more higher-order term in the functions of p and V.

Fig. 3 shows $V(\lambda)$ for both cases of $k' = 2, 3$ and 4, which exhibit the minimum at $\lambda = 1$. Note that because the undeformed bond length l_p^u is corresponding to different λ^u, the zero-force bond lengths are different for the three cases. With k' increase from 2 to 4, λ^u decrease from 1.1444 to 1.1199. For $\lambda < 1$, it increases faster in comparison with $\lambda > 1$, which represents a larger repulsive force than the attactive force with the same change of stretch level. When k' increases, the interatomic potential well becomes stiffer.

Using the derivatives of $\overline{V}_{,\lambda}(\lambda)$ and $\overline{V}_{,\lambda\lambda}(\lambda)$ of Eq. (57) for Case $k' = 2$, we can predict the elastic constants changing with λ or pressure. Fig. 4 illustrates the three cubic symmetric elastic

constants changing with λ. Indeed, at the undeformed state, the predictions of the three elastic constants are the same as the measurements because the potential was determined by those values. With the increase of λ, the elastic constants reduce at different rates: c_{44} changes much slower than c_{11} and c_{12}. Note that here the range of λ from 0.9-1.2 covers a large range of the volume change and is far beyond the engineering applications. When λ is close to 0.9, the trend may not be physical as the elastic constants exhibit the peak points.

Mechanics and physics of crystals predicted by the improved singum model

In the last subsection, single crystalline aluminum was used for demonstration. The improved singum model provides a practical approach to correlate the EOS with the interatomic potential and elastic constants at different volume or bond length or pressure.

The key novelty of the singum model is to take into account of the effect of the prestress on the effective stiffness, which generates a configurational force with a displacement variation on the lattice structure and changes the effective elasticity significantly. If the prestress reduces to zero, which means that the undeformed bond length stays at the bottom of the potential well, which is equal to the equilibrium bond length, for short-range atomic interactions, the singum model provides the same formulation as other models. For example, replacing the interatomic potential by the Hertzian contact model, the singum model recovers Chang's formulation (Chang 1988) using $V_{,r} = 0$. For 3D isotropic cases, previous models typically led to a Poisson's ratio at 0.25 using the pairwise potential without prestress, which is shown in the Singum model as well. However, the compressive prestress makes the Poisson's ratio higher than 0.25 and a tensile prestress makes it less than 0.25, which has been demonstrated by the singum model recently (Yin 2022b).

Compared with microcanonical (NVE) ensemble (Tadmor and Miller 2011), the simplified singum uses the static lattice geometry to map the stress in a space with forces between atoms. Although only neighboring atomic interactions in a short range is considered and the temperature effect with kinetic energy is not taken into account, the improved singum model can catch the mechanics and physics of the solids that NVE ensemble does not take into account as the following features:

1. In general, NVE requires the statistical equilibrium of the forces. If only short-range atomic interactions are considered, it means all bonds shall stay at the zero-force bond length l_p^0 statistically at the undeformed state, which eliminates the second and third terms in Eq. (32). Actually, solids exhibit surface energy which can change the state shifted from the lowest potential state. We use prestress to explain it. It will produce configurational forces with the displacement variation and play a significant role in elastic behavior, which has been explained in the second paper about metamaterial (Yin 2022a).

2. Indeed, if $V_{,\lambda}$ becomes zero, the singum model will lead to Cauchy discrepancy (Daw and Baskes 1984; Tadmor and Miller 2011), where $c_{11} = 2c_{12} = 2c_{44}$ in Eq. (36). However, the prestress changes the elastic behavior with the configurational forces.

3. If no long-range atomic interactions are considered, the FCC atomic system per pairwise interaction can be simulated by a lattice metamaterial with equal bond lengths. The singum model shows $2c_{11} = c_{12} + 3c_{44}$, which is exact for lattice metamaterial but not physical for FCC crystals due to the long-range atomic interactions.

4. When the long-range atomic interactions are approximated by a pressure function which is similar to embedding energy of the EAM, the improved singum model can fit the elastic constants well with a predefined form of EOS. The elastic constants changing with pressure can be subsequently determined.

5. As discussed in the first paper (Yin 2022b), if the undeformed state exhibits a bond length l_p^u larger than l_p^0, it is generally brittle; whereas if $l_p^u < l_p^0$, it is generally ductile as it requires more energy to separate the atoms. Using the present formulation with finite deformation under hydrostatic loading, we can predict the nonlinear elastic behavior of the singum (Wei et al. 2009) and investigate the elastoplastic and fracture behavior of the solids.

6. Although only pair interactions are considered, the improved singum model can predict the general anisotropic elastic properties of central symmetric lattice, which is different from the general view that 3-body or N-body interatomic potential is needed to catch the arbitrary cubic symmetric elastic behavior (Tadmor and Miller 2011).

This is the third paper about the singum model following the two recent papers (Yin 2022b; Yin 2022a). The first paper (Yin 2022b) introduced the construction of the singum particle and provided some preliminary applications of the simplified singum model based on the infinitesimal deformation. Because the formulation cannot interpret the three independent elastic constants of cubic symmetric lattice, and it was abstractive and difficult to justify the interatomic potential by curve fitting, the second paper (Yin 2022a) used the physical truss system with harmonic potential to demonstrate the singum model. It provided an analytical form of elasticity for lattice metamaterials and clarified the effect of the prestress on the elasticity. However, it was still based on the infinitesimal deformation. This paper revisits the crystal lattices using FCC for demonstration, which can be straightforwardly extended to other types of lattices, and develops the finite deformation formulation. Therefore, it will be more accurate in nonlinear elastic modeling of the crystal solids or lattice metamaterials and composites under large deformation.

In addition, the present singum model disregards the thermal effects of atom vibration. On the scale of atoms, the thermal fluctuation can be random and evaluated by the statistical mechanics of a many-particle system (Tadmor and Miller 2011). The effect of kinetic and fluctuation contributions to the elasticity can be considerable although the Cauchy-Born's part, on which the preent singum model focuses, still plays the dominant role. In this work, because only short-range interactions with a few atoms are considered, we calibrated the potential function with experimental results of the stiffness and density so that the temperature effect is not separately analyzed. However, when long-range atomic interactions are considered in future, we can investigate the thermal effects in a quantitative way.

Note that the present singum model keeps the shape of unit cell the same as a cube, so that the singum particle exhibits the same out-norm vector $\mathbf{n}^I$ of each surface, although the full anisotropic stiffness tensor is obtained by applying a displacement variation. Indeed, the shape of the singum remains the same under the hydrostatic load, and the EOS is obtained by the finite deformation under a hydrostatic pressure. However, for general finite deformation, such as shear loading, the surface out-norm vector $\mathbf{n}^I$ of each surface has to be updated with the deformation, so that the formulation

shall be updated with the load and the explicit form of the elastic constants of the present paper will be lost. Instead, the equivalence between the interatomic potential and the Helmholtz free energy can be setup on the singum and the general finite deformation of the crystal lattices (Wei et al. 2009; Kumar and Parks 2015; Höller et al. 2020) can be formulated. The actual loading curves can be generated incrementally with the lattice structure evolution, which may lead to elasto-plastic or fracture behavior with the singum annihilation and transformation when the closest neighbor atoms are changed (Yin 2022b). Future work on the lattice large deformation is underway.

CONCLUSIONS

The simplified singum model has been improved by using the thermodynamics-based equation of state (EOS) of solids and approximately considering the long-range atomic interactions. The finite deformation formulation has been developed to evaluate the pressure-volume (p-v) relationship for the EOS of a solid, and predict the elastic constants changing with the bond length or pressure. Using the bulk modulus and its derivatives at the free-stress state, one can construct the EOS and interatomic potential. Using single crystalline aluminum as an example, the improved singum model is demonstrated. The third-order EOS can predict the p-v curve up to a pressure of 100GPa. The pressure dependent elastic behavior is predicted with the improved singum model. The mechanics and physics of crystals caused by surface energy and long-range atomic interactions are discussed, which can be useful for elastoplastic and fracture modeling of solids.

DATA AVAILABILITY STATEMENT

All data that support the findings of this study are available from the corresponding author upon reasonable request.

ACKNOWLEDGEMENT

This work is sponsored by the National Science Foundation IIP #1738802, IIP #1941244, CMMI #1762891, and U.S. Department of Agriculture NIFA #2021-67021-34201, whose support is gratefully acknowledged. The author thanks Dr. Jeffrey Kysar and Dr. Sinan Keten for the

helpful discussion and the sharing of their relevant papers. This work was inspired by Dr. Richard Li's PhD dissertation, and Junhe Cui has conducted careful reading and found several typos.

REFERENCES

Bazant, Z. P. and Cedolin, L. (2010). *Stability of structures: elastic, inelastic, fracture and damage theories*. World Scientific.

Birch, F. (1947). "Finite elastic strain of cubic crystals." *Physical review*, 71(11), 809.

Birch, F. (1952). "Elasticity and constitution of the earth's interior." *Journal of Geophysical Research*, 57(2), 227–286.

Chang, C. (1988). "Micromechanical modelling of constitutive relations for granular material." *Studies in Applied Mechanics*, Vol. 20, Elsevier, 271–278.

Chen, L.-R. and Chen, Q.-H. (1991). "The test and comparison of three equations of state for solids." *Communications in Theoretical Physics*, 16(4), 385.

Chen, W. and Fish, J. (2006). "A mathematical homogenization perspective of virial stress." *International journal for numerical methods in engineering*, 67(2), 189–207.

Cohen, R. E., Gulseren, O., and Hemley, R. J. (2000). "Accuracy of equation-of-state formulations." *American Mineralogist*, 85(2), 338–344.

Daw, M. S. and Baskes, M. I. (1984). "Embedded-atom method: Derivation and application to impurities, surfaces, and other defects in metals." *Physical Review B*, 29(12), 6443.

Dewaele, A., Loubeyre, P., and Mezouar, M. (2004). "Equations of state of six metals above 94 gpa." *Physical Review B*, 70(9), 094112.

Ericksen, J. (2008). "On the cauchy—born rule." *Mathematics and mechanics of solids*, 13(3-4), 199–220.

Fürth, R. (1944). "On the equation of state for solids." *Proceedings of the Royal Society of London. Series A. Mathematical and Physical Sciences*, 183(992), 87–110.

Guinan, M. W. and Steinberg, D. J. (1974). "Pressure and temperature derivatives of the isotropic polycrystalline shear modulus for 65 elements." *Journal of Physics and Chemistry of Solids*, 35(11), 1501–1512.

Hama, J. and Suito, K. (1996). "The search for a universal equation of state correct up to very high pressures." *Journal of Physics: Condensed Matter*, 8(1), 67.

Höller, R., Smejkal, V., Libisch, F., and Hellmich, C. (2020). "Energy landscapes of graphene under general deformations: Dft-to-hyperelasticity upscaling." *International Journal of Engineering Science*, 154, 103342.

Holzapfel, W., Hartwig, M., and Sievers, W. (2001). "Equations of state for cu, ag, and au for wide ranges in temperature and pressure up to 500 gpa and above." *Journal of Physical and Chemical Reference Data*, 30(2), 515–529.

Hutter, K. and Jöhnk, K. (2013). *Continuum methods of physical modeling: continuum mechanics, dimensional analysis, turbulence*. Springer Science & Business Media.

Jarvis, S., Yamada, H., Yamamoto, S.-I., Tokumoto, H., and Pethica, J. (1996). "Direct mechanical measurement of interatomic potentials." *Nature*, 384(6606), 247–249.

Jiménez Segura, N., Pichler, B. L., and Hellmich, C. (2022). "Stress average rule derived through the principle of virtual power." *ZAMM-Journal of Applied Mathematics and Mechanics/Zeitschrift für Angewandte Mathematik und Mechanik*.

Johnson, R. (1972). "Relationship between two-body interatomic potentials in a lattice model and elastic constants." *Physical Review B*, 6(6), 2094.

Juvé, V., Crut, A., Maioli, P., Pellarin, M., Broyer, M., Del Fatti, N., and Vallée, F. (2010). "Probing elasticity at the nanoscale: terahertz acoustic vibration of small metal nanoparticles." *Nano letters*, 10(5), 1853–1858.

Kumar, S. and Parks, D. M. (2015). "On the hyperelastic softening and elastic instabilities in graphene." *Proceedings of the Royal Society A: Mathematical, Physical and Engineering Sciences*, 471(2173), 20140567.

Ming, P. et al. (2007). "Cauchy–born rule and the stability of crystalline solids: static problems." *Archive for rational mechanics and analysis*, 183(2), 241–297.

Mishin, Y. (2021). "Machine-learning interatomic potentials for materials science." *Acta Materialia*, 214, 116980.

Mura, T. (1987). *Micromechanics of defects in solids*. Springer Netherlands.

Murnaghan, F. D. (1937). "Finite deformations of an elastic solid." *American Journal of Mathe-*

matics, 59(2), 235–260.

Occelli, F., Loubeyre, P., and LeToullec, R. (2003). "Properties of diamond under hydrostatic pressures up to 140 gpa." *Nature materials*, 2(3), 151–154.

Ruiz, L., Xia, W., Meng, Z., and Keten, S. (2015). "A coarse-grained model for the mechanical behavior of multi-layer graphene." *Carbon*, 82, 103–115.

Shukla, M. (1981). "Comment on "relationship between two-body interatomic potentials in a lattice model and elastic constants"." *Physical Review B*, 23(10), 5615.

Swift, D. C., Heuzé, O., Lazicki, A., Hamel, S., Benedict, L. X., Smith, R. F., McNaney, J. M., and Ackland, G. J. (2022). "Equation of state and strength of diamond in high-pressure ramp loading." *Physical Review B*, 105(1), 014109.

Tadmor, E. B. and Miller, R. E. (2011). *Modeling materials: continuum, atomistic and multiscale techniques*. Cambridge University Press.

Vallin, J., Mongy, M., Salama, K., and Beckman, O. (1964). "Elastic constants of aluminum." *Journal of Applied Physics*, 35(6), 1825–1826.

Vinet, P., Ferrante, J., Smith, J., and Rose, J. (1986). "A universal equation of state for solids." *Journal of Physics C: Solid State Physics*, 19(20), L467.

Vinet, P., Rose, J. H., Ferrante, J., and Smith, J. R. (1989). "Universal features of the equation of state of solids." *Journal of Physics: Condensed Matter*, 1(11), 1941.

Voronoi, G. (1908). "Re echerches sur les parall elo edres primitifs i, ii." *J. reine angew. Math*, 134, 198–287.

Wei, X., Fragneaud, B., Marianetti, C. A., and Kysar, J. W. (2009). "Nonlinear elastic behavior of graphene: Ab initio calculations to continuum description." *Physical Review B*, 80(20), 205407.

Wigner, E. and Seitz, F. (1933). "On the constitution of metallic sodium." *Physical Review*, 43(10), 804.

Yin, H. (2022a). "Generalization of the singum model for the elasticity prediction of lattice meta-materials and composites." *ASCE Journal of Engineering Mechanics*, (in press).

Yin, H. (2022b). "A simplified continuum particle model bridging interatomic potentials and

elasticity of solids." *Journal of Engineering Mechanics*, 148(5), 04022017.

Yin, H. and Zhao, Y. (2016). *Introduction to the micromechanics of composite materials*. CRC press.

Zhou, M. (2003). "A new look at the atomic level virial stress: on continuum-molecular system equivalence." *Proceedings of the Royal Society of London. Series A: Mathematical, Physical and Engineering Sciences*, 459(2037), 2347–2392.

Zuo, Y., Chen, C., Li, X., Deng, Z., Chen, Y., Behler, J., Csányi, G., Shapeev, A. V., Thompson, A. P., Wood, M. A., et al. (2020). "Performance and cost assessment of machine learning interatomic potentials." *The Journal of Physical Chemistry A*, 124(4), 731–745.

List of Figures

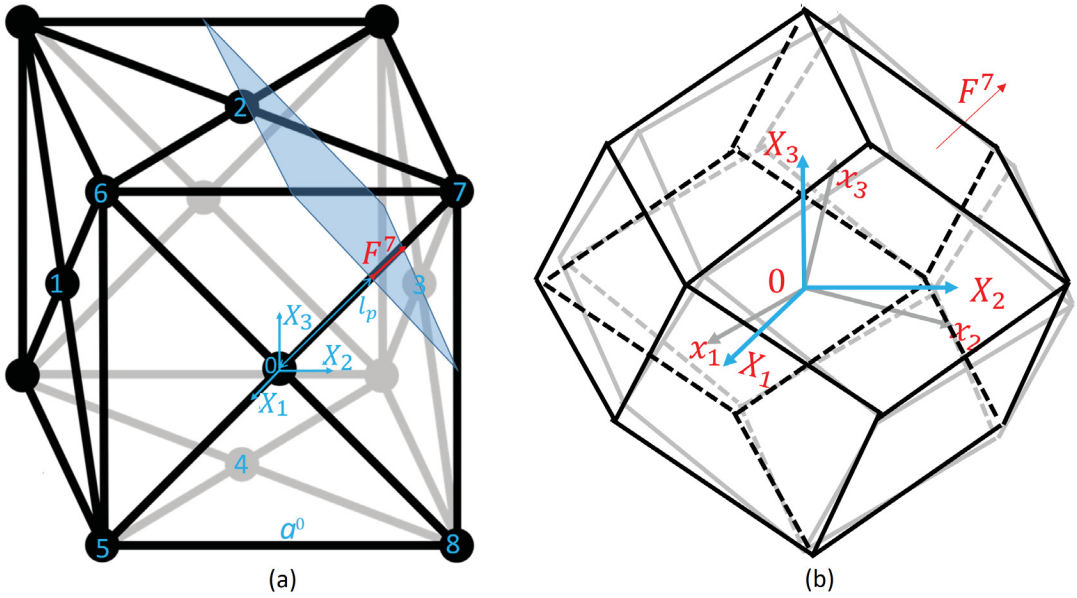

Fig. 1. The singum model of a face-centered cubic lattice: (a) the unit cell for the singum construction at the front central atom with four more member atoms not shown and; (b) the FCC singum of the 0^{th} atom obtained by cutting the 12 bonds with the vertical midplanes, which is the WS Cell of a rhombic dedecahedron shown in the initial configuration **X** (black lines) and the deformed configuration **x** (gray lines)

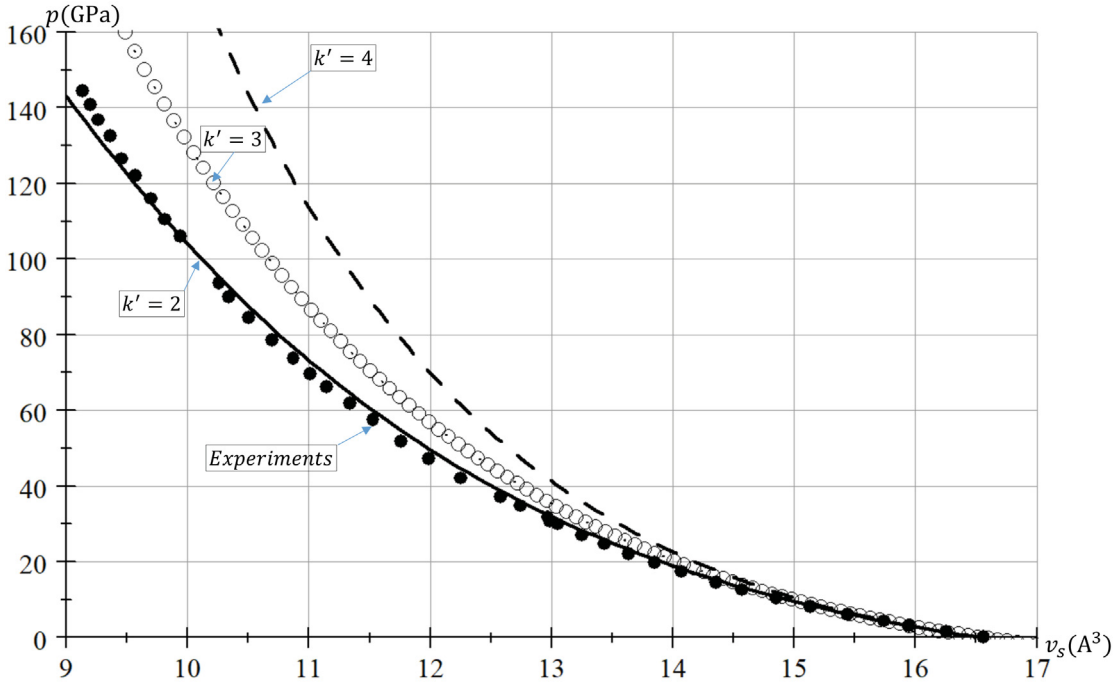

Fig. 2. The pressure changing with the singum volume (p-v) in comparison with the experiments of single crystalline aluminium: circle symbols - experiments (Dewaele et al. 2004); dash line for $k' = 4$ - second order EOS Eq. (15); solid line for $k' = 2$; dot symbols for $k' = 3$, and; dot line for $k' = 5$

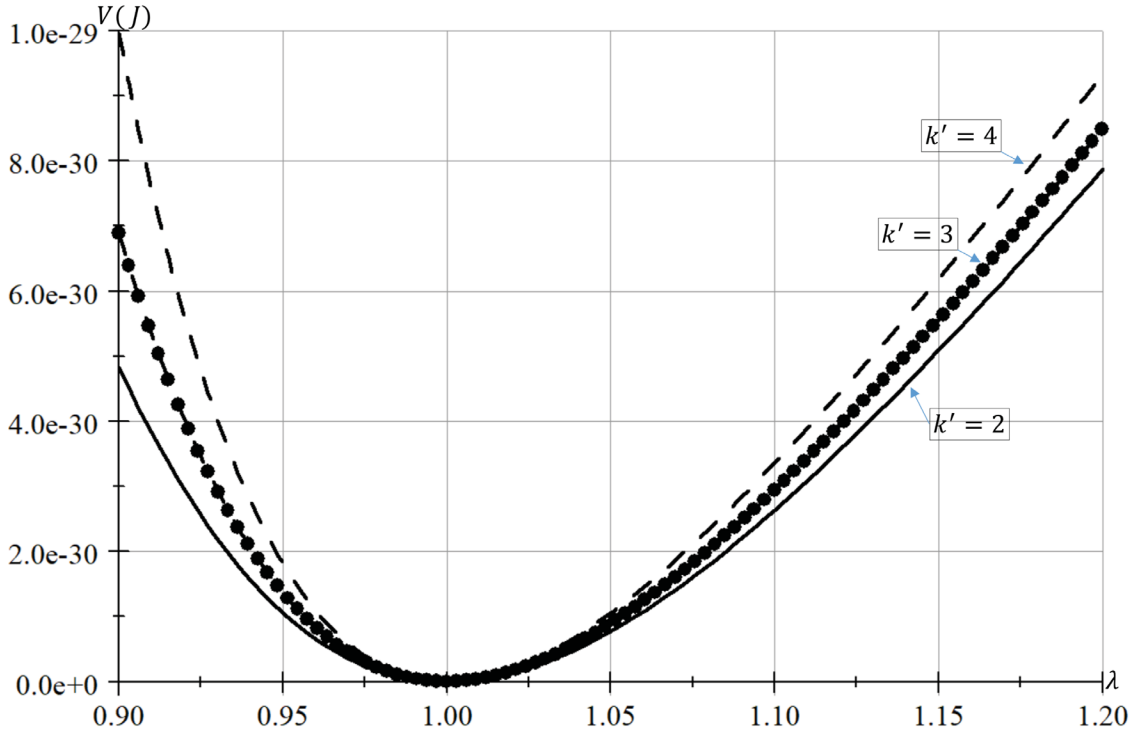

Fig. 3. The interatomic potential of the singum model for a face-centered cubic lattice of single crystalline aluminium: dash line for $k' = 4$ - second order EOS Eq. (15); solid line for $k' = 2$ - third order EOS Eq. (17)

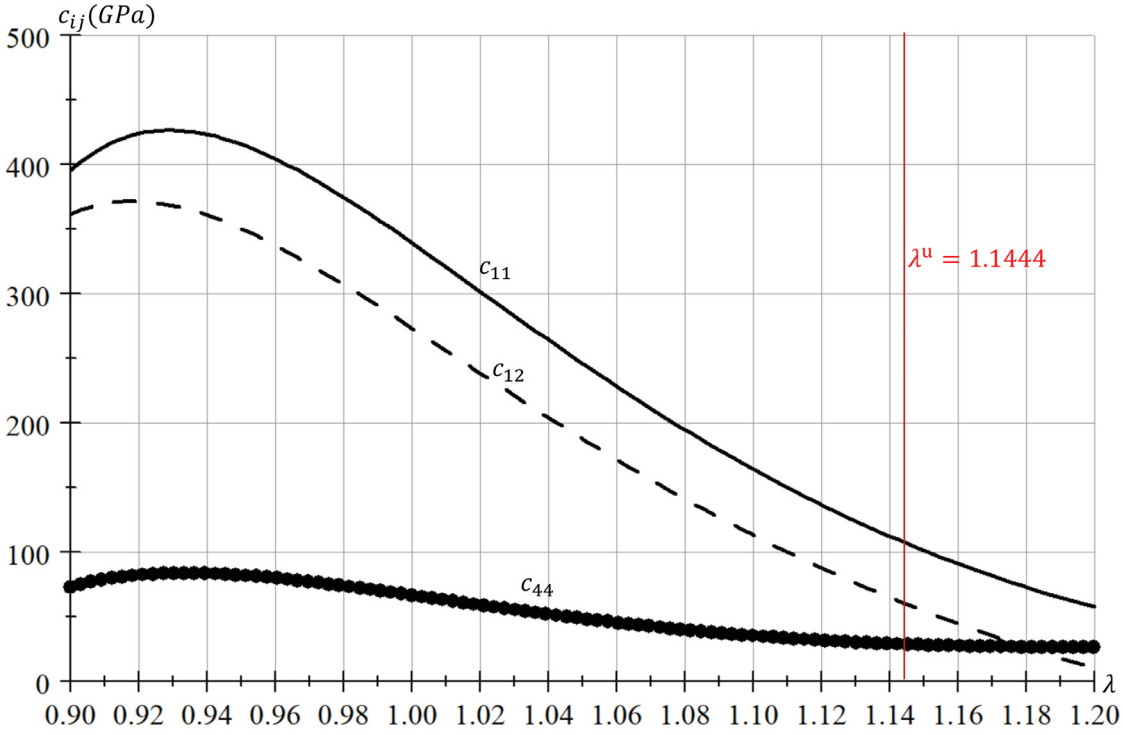

Fig. 4. The three elastic constants of single crystalline aluminium changing with λ, where λ^u indicates the undeformed state